Supporting Information

Self-Assembled Tri-, Tetra- and Penta-Ethylene Glycols as an Easy, Expedited and Universal Interfacial Cathode-Modifier for Inverted Polymer Solar Cells

Fong-Yi Cao, Yu-Ying Lai, Yung-Lung Chen, and Yen-Ju Cheng*

Department of Applied Chemistry, National Chiao Tung University, 1001 University Road, Hsin-Chu, 30010 Taiwan.

E-mail: yjcheng@mail.nctu.edu.tw

The condition of the blending solution for the device fabrication

Table S1. The condition of the blending solution with PBDTTT-EFT, PBDT-TS1, PBDCPDT-FBT, PBDCPDT-TPD, PDPP3T and P3HT as the donor.

Blending system (donor/acceptor)	Blending ratio in wt%	Conc.	Solvent	Additive	Thermal annealing	Spin rate (rpm)
PBDTTT-EFT/ $PC_{71}BM$	1:1.5	15 mg/ml	*o*-DCB	3 v% DIO	x	1700
PBDT-TS1/ $PC_{71}BM$	1:1.5	8 mg/ml	CB	3 v% DIO	x	1000
PBDCPDT-FBT/ $PC_{71}BM$	1:3	6 mg/ml	*o*-DCB	x	150 °C 15 min	800
PBDCPDT-TPD/ $PC_{71}BM$	1:3	6 mg/ml	*o*-DCB	x	150 °C 15 min	800
PDPP3T/ $PC_{71}BM$	1:2	6 mg/ml	*o*-DCB/ CF (3:1)	3 v% DIO	x	1000
P3HT/$PC_{61}BM$	1:1	20 mg/ml	*o*-DCB	x	100 °C 10 min	600

o-DCB: *ortho*-dichlorobenzene.
DIO: 1,8-diiodooctane

Water contact angle measurements

Table S2. Water contact angle measurement of ITO and SA-EG modified ITO surface

Sample	ITO	ITO/3-EG	ITO/4-EG	ITO/5-EG
CA (°)	2	24	23	22
	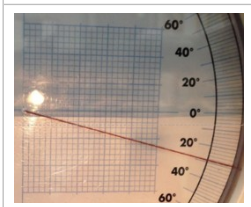	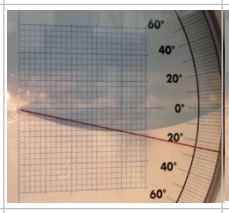	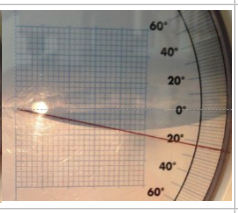	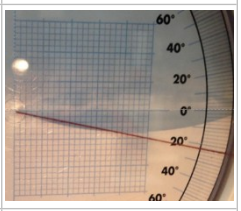
CA (°)[a]	-	20	22	20
	-	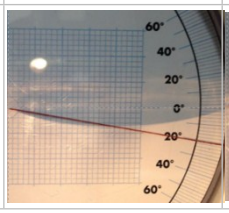	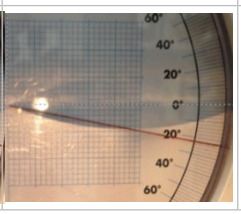	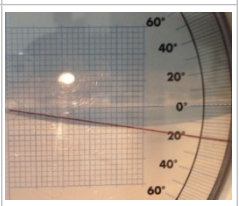

[a]after spin rinsing with *o*-DCB, CA is contact angle.

Atomic force microscopy measurements

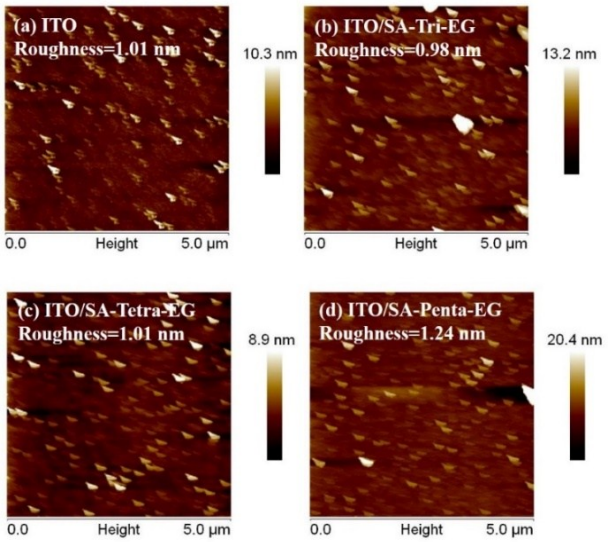

Figure S1. AFM tapping mode height images of the surface of (a) bare ITO, (b) 3-EG/ITO, (c) 4-EG/ITO, (d) 5-EG/ITO.

Optical transmittance spectra

The transmittance of the SA-EG modified ITO glasses is shown in the Figure S2. All the samples showed the high transmittance of 93% in the visible region. These results display that the introduction of the SA-EG layer can modulate the W_F of the ITO surface and keep the high optical transparency of the ITO.

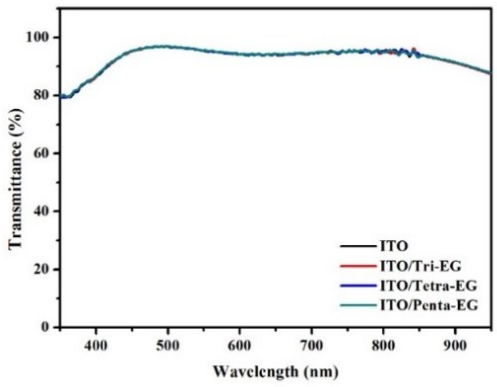

Figure S2. Optical transmittance of the ITO, ITO/3-EG, ITO/4-EG, and ITO/5-EG.

EQE spectra

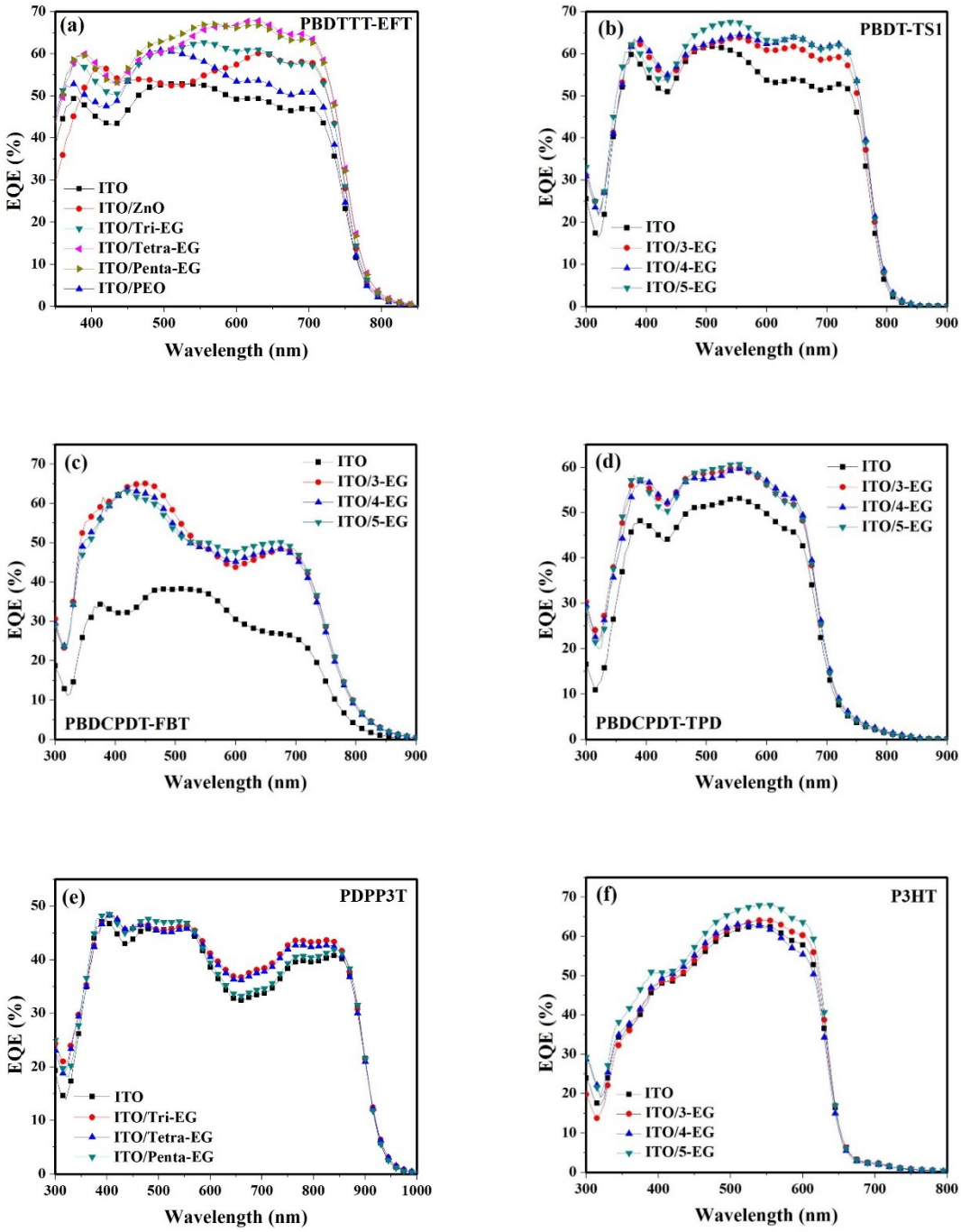

Figure S3. EQE spectra of devices with different polymer donors (a) PBDTTT-EFT (b) PBDT-TS1 (c) PBDCPDT-FBT (d) PBDCPDT-TPD (e) PDPP3T (f) P3HT.

Computational details

Geometry optimization was performed with the Gaussian09 suite[S1] employing the CAM-B3LYP density functional in combination with the LanL2DZ basis set for Sn and In and the 6-311G(d,p) for the remaining atoms. SITO was first geometry-optimized and the optimized SITO structure was then used as frozen coordinates for the rest optimization, meaning the structural reorganization of SITO upon interacting with 2-EG is not taken into account. HOMO/LUMO energy was obtained from the single-point calculation of the optimized geometry with the ADF suite[S2-S4] using BP86-BJDAMP[S5]/TZP density including relativistic scalar zora. ETS-NOCV analysis was performed with the ADF suite under the same level of theory.

"Based on the ETS NOCV method, the net bonding energy ΔE consists of two contributions: the preparation energy ΔE_{prep} required to deform the separate fragments from their equilibrium structure to their geometries in the total molecule and to excite them to their valence electronic configurations; and the interaction energy ΔE_{int} between the fragments, which is further decomposed into three chemically meaningful components, ΔV_{elst}, ΔE_{pauli}, and ΔE_{oi}. ΔV_{elst} is the classical electrostatic interaction between the fragments as they are brought to their positions in the final complex. ΔE_{pauli} refers to the repulsive Pauli interaction between occupied orbitals of different fragments in the final molecule. ΔE_{oi} represents the stabilizing interactions between the occupied molecular orbitals on one fragment and the unoccupied molecular orbitals on the other fragment as well as mixing of occupied and virtual orbitals within the same fragment after the two fragments have been brought

together. An atom pair-wise additive treatment of the dispersion energy is included in BP86-BJDAMP. An additional energy component, dispersion energy (ΔE_{dis}) is therefore integrated into the interaction energy ΔE_{int}.

$$\Delta E_{net} = \Delta E_{prep} + \Delta E_{int} \quad (1)$$

$$\Delta E_{int} = \Delta V_{elst} + \Delta E_{pauli} + \Delta E_{oi} + \Delta E_{dis} \ (2)$$"[S6]

REFERENCES

S1 Gaussian 09, Revision ***A.1***, Frisch, M. J.; Trucks, G. W.; Schlegel, H. B.; Scuseria, G. E.; Robb, M. A.; Cheeseman, J. R.; Scalmani, G.; Barone, V.; Mennucci, B.; Petersson, G. A.; Nakatsuji, H.; Caricato, M.; Li, X.; Hratchian, H. P.; Izmaylov, A. F.; Bloino, J.; Zheng, G.; Sonnenberg, J. L.; Hada, M.; Ehara, M.; Toyota, K.; Fukuda, R.; Hasegawa, J.; Ishida, M.; Nakajima, T.; Honda, Y.; Kitao, O.; Nakai, H.; Vreven, T.; Montgomery, J. A. Jr.; Peralta, J. E.; Ogliaro, F.; Bearpark, M.; Heyd, J. J.; Brothers, E.; Kudin, K. N.; Staroverov, V. N.; Kobayashi, R.; Normand, J.; Raghavachari, K.; Rendell, A.; Burant, J. C.; Iyengar, S. S.; Tomasi, J.; Cossi, M.; Rega, N.; Millam, J. M.; Klene, M.; Knox, J. E.; Cross, J. B.; Bakken, V.; Adamo, C.; Jaramillo, J.; Gomperts, R.; Stratmann, R. E.; Yazyev, O.; Austin, A. J.; Cammi, R.; Pomelli, C.; Ochterski, J. W.; Martin, R. L.; Morokuma, K.; Zakrzewski, V. G.; Voth, G. A.; Salvador, P.; Dannenberg, J. J.; Dapprich, S.; Daniels, A. D.; Farkas, O.; Foresman, J. B.; Ortiz, J. V.; Cioslowski, J. and Fox, D. J. Gaussian, Inc., Wallingford CT, 2009.

S2 te Velde, G.; Bickelhaupt, F. M.; van Gisbergen, S. J. A.; Fonseca Guerra, C.; Baerends, E.J.; Snijders, J.G.; Ziegler, T. J. Chemistry with ADF. *Comput. Chem.*, 2001, **22**, 931.

S3 Fonseca Guerra, C.; Snijders, J.G.; te Velde, G.; Baerends, E.J. Towards an Order-N DFT Method. *Theor. Chem. Acc.*, 1998, **99**, 391.

S4 ADF2014, SCM, Theoretical Chemistry, Vrije Universiteit, Amsterdam, The Netherlands, http://www.scm.com

S5 Grimme, S.; Ehrlich, S.; Goerigk, L. Effect of the Damping Function in Dispersion Corrected Density Functional Theory. *J. Comput. Chem.*, 2011, **32**, 1456.

S6 Liao, M.-H.; Tsai, C.-E.; Lai, Y.-Y.; Cao, F.-Y.; Wu, J.-S.; Wang, C.-L.; Hsu, C.-S.; Liau, I.; Cheng, Y.-J. Morphological Stabilization by Supramolecular Perfluorophenyl-C60 Interactions Leading to Efficient and Thermally Stable Organic Photovoltaics. *Adv. Funct. Mater.*, 2014, **24**, 1418–1429.